Coherence and volumetric curvatures and their spatial relationship to faults and folds, an example from Chicontepec basin, Mexico

Ha T. Mai, Kurt J. Marfurt, University of Oklahoma, Norman, USA, Sergio Chávez-Pérez, Instituto Mexicano del Petróleo*

Summary

Geometric attributes such as coherence and volumetric curvature are commonly used in delineating faults and folds. While fault patterns seen in coherence, most-positive curvature and most-negative curvature are easily recognized on time slices, they are often laterally shifted from each other. The kind and degree of lateral shift is an indication of the underlying tectonic deformation. In this tutorial, we document some of these relationships when applied to the structurally-complex section within the Chicontepec Basin, Mexico.

Introduction

While coherence attributes measure lateral changes in the waveform and allow us to map reflector offsets, lateral changes in stratigraphy, and chaotic depositional features, volumetric curvature attributes measure lateral changes in dip magnitude and dip azimuth, and are thus allows us to map folds, flexures, buildups, collapse features, and differential compaction. Both attributes are used widely in detecting faults with each attribute has its advantages and disadvantages. Coherence accurately tracks vertical faults cutting coherent seismic reflectors. For dipping faults, coherence exhibits a vertically-smeared stair-step appearance, due to most implementations being computed on vertical seismic traces. Where there is fault drag, or sub-seismic resolution anithetic faulting that appears as fault drag, coherence may not illuminate the fault at all. For faults with very small displacement, the reflectors appear to have subtle change in dip, have no coherence anomaly, and rather appear as a slight flexure which appears as a curvature anomaly. For faults having significan offset, curvature anomalies track the folds on either side of a fault, where drag, antithetic faulting, or syntectonic deposition results in slightly folded reflectors. For this reason, curvature anomalies often do not align with faults.

Since faults are often more easily visualized on attribute time slices, we will use a complexly folded and faulted survey acquired in the Chinconetepec Basis, Mexico, to illustrate some of these interpretational features..

Theory

Curvature in 2D is defined by the radius of a circle tangent to a curve (Figure 1, after Roberts, 2001). In 3D, we need to fit two circles tangent to a surface (Figure 2). The circle with minimum radius is the maximum curvature (k_{max}) and the circle with maximum radius is the minimum curvature (k_{min}). In relation to geology, anticlinal features will have positive maximum curvature, and a synclinal feature will have negative maximum curvature.

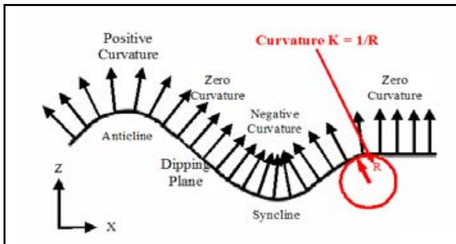

Figure 1: An illustrated definition of 3D curvature. Synclinal features have negative curvature and anticlinal fearures have positive curvature

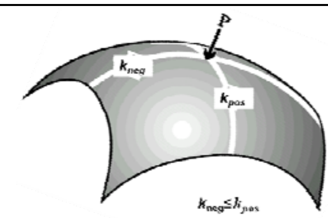

Figure 2: Most-positive and most-negative curvatures (Modified from Lisle, 1994)

The interpretation of curvature volumes computed over folded geologies is straightforward. For anticlines, we see a positive curvature lineament along the fold axis and two negative curvature lineaments at the limbs. For synclines, we see a negative curvature lineament along the fold axis and two positive curvature lineaments along the limbs (Figure 3). Since the layers are continuous, the waveform is also continuous along the fold, such that discontinuity

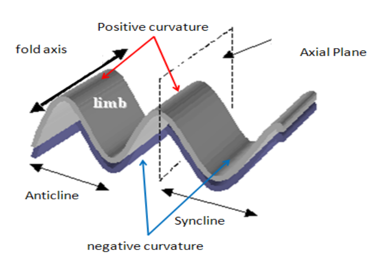

Figure 3: Illustration of fold with positive and negative curvature.

measurements such as coherence do not show any anomalies.

The attribute expression of faults can be considerably more complicated. For normal faults with vertical displacements greater than half a seismic wavelength, we often see a discrete discontinuity that is clearly delineated by a low coherence lineament. For highly competent rocks we may see no curvature anomalies associated with a simple normal fault. However, more commonly we see drag on either side of the fault, which may be either through plastic deformation or through a suite of conjugate faults. Parallel to the fault strike, we often have ramp structures. For an excellent outcrop analysis of such features we direct the reader to a recent publication by Ferrill and Morris (2008). A schematic of curvature associated with normal faults is shown in Figure 4.

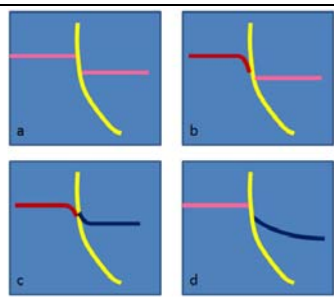

Figure 4: An illustration of normal faults with positive and negative curvature: (a) simple displacement with no drag, (b) fault with drag on one side, (c) fault with drag on two sides, and (d) fault with syntectonic depositions.

Listric faults geometries associated with syntectonic deposition can be considerably more complicated. On the footwall, we may see very little deformation, with the sediments maintaining their original attitude at some angle to the fault face. On the hanging wall, the reflectors rotate with depth, often maintaining a near-normal relation to the fault face. We may also see a positive curvature anomaly over the roll-over anticline if one exists. Coherence does a good job of delineating the fault dislocation. Deeper in the section, as the fault begins to sole out, both coherence and curvature images become noisy and less easily interpreted.

Alternative definitions of maximum and minimum curvature

Most references (in both mathematics and geology) define the maximum curvature to be the tightest (highest absolute value) of the two principal curvatures, k_1 and k_2:

$$k_{max} = k_1 \text{ and } k_{min}=k_2, \text{ if } |k_1| > |k_2|$$

$$k_{max} = k_2 \text{ and } k_{min}=k_1, \text{ if } |k_2| > |k_1|.$$

Many interpreters find this definition to be an effective means of mapping fault throw from time slices (e.g. Sigisumundi and Soldo, 2003). However, other workers (e.g. Rich, 2008) find it to be interpretationally useful to define k_{max} = MAX(k_1,k_2) and k_{min} = MIN(k_1,k_2).

The second author has long favored most-positive and most-negative curvature since they provide images of karst and differential compaction that are interpretational simpler to understand. Rich (2008) points out that this 2nd (less common) definition, produces images similar to most-positive and most-negative curvature, but take account of the reflector rotation.

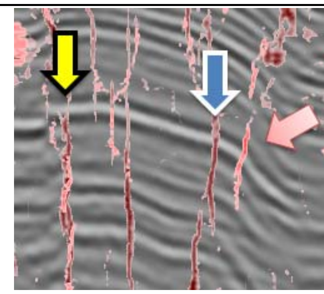

Figure 5: Ant-tracking on most-positive curvature (red, with blue arrow) and on new defined maximum curvature (pink, with pink arrow).

Figure 5 shows the results of ant-tracking applied to most-positive and the newly-defined maximum curvature. The latter shows the axis of a dipping flexure (pink arrow) while the most-positive shows the axis of a less geologically-interesting fold with respect to the horizontal. In gently dipping areas such as in the Fort Worth Basin, k_{max} and k_{pos} are nearly identical (Figure 5, yellow arrow).

Example from Chicontepec basin, Mexico

In order to illustrate the lateral relationship of our new definitions of maximum and minimum curvature with and coherence, we use 3D seismic data from Amatitlán, Chicontepec basin.

Multiple volumetric attributes (k_{pos}, k_{neg}, k_{max}, k_{min}, ψ_{min}, energy ratio coherence, and variance) were calculated from the seismic volume. Where indicated in the captions, a commercial "ant-tracking" image processing algorithm was applied to the attributes to "skeletonize" the image, thereby increasing the visual continuity for interpretation purposes.

Figure 6 shows an anticlinal feature. Since there is no interruptions present along the interpreted horizon (white dashed line), there are no significant coherence anomalies present. However, the dip does change along the horizon such that we see maximum curvatures anomalies along the fold axis, and minimum curvature anomalies along the fold limbs.

Coherence and volumetric curvatures and their spatial relationship to faults and folds, an example from Chicontepec basin, Mexico

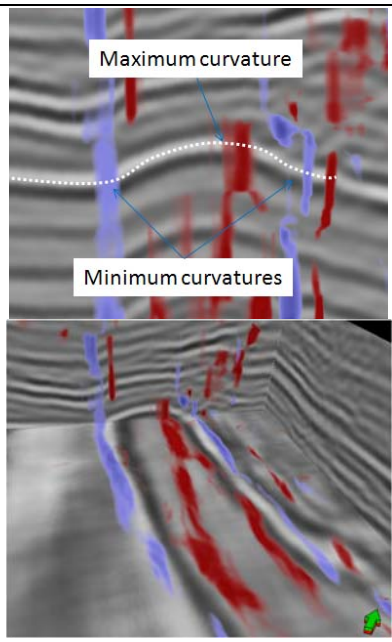

Figure 6: Anticlinal feature. Minumum curvature features (blue) delineate the two limbs of the fold, while maximum curvature (red) delineate the axial plane.. There are no significant coherence anomalies.

For fault features, the interpretation is much more complicated. Figures 7 and 9 show several reverse fault features. We note a center pop-up block, with the reflectors bent down along the east side of the west fault. The maximum curvature anomaly appears to the right of the coherence anomaly (Figure 7, red arrow). To the west side of the fault, due to fault drag, the curvature anomaly is broader, with the minimum curvature anomaly a some distance from the fault, as well as from maximum curvature and coherence anomalies. Figure 9 shows the same features, with coherence, maximum and minimum curvatures on vertical and time slices. Following the fault to the east, the minimum curvature lineament approaches to the most-positive curvature lineament, indicating folding or drag, creating a pair of maximum/minimum curvatures with coherence in the middle, thereby defining the fault.

Figures 8 and 10 shows normal faults delineating a graben. Again, we see a pair of maximum curvature and coherence next to each other, and a minimum curvature lineament at a distance. This are the same geometries discussed by Sigusmondi and Soldo (2003). Vertically, the curvatures appear to be more continuous, and more easily interpreted than the coherence anomaly which tends to be discontinuous and vertically smeared.

Conclusions

Discontinuity measurements such as coherence are not sensitive to smooth folding, and often result in anomalies that are discontinuous when viewed in the vertical section. Where they are not vertically smeared, they accurately locate the discontinuity. In contrast, curvature lineaments are more continuous on the vertical section and maps folds and flexures. With fault drag and/or antithetic faulting, volumetric curvature will commonly bracket faults with maximum and minimum anomalies but does not give exact fault location. Co-rendering curvature with coherence along with the seismic amplitude data provides a superior interpretation product.

Acknowledgments

We thank PEMEX Exploración y Producción for permission to publish this work and particularly to Juan M. Berlanga, Proyecto Aceite Terciario del Golfo, PEMEX Exploración y Producción, for making our work possible through access to seismic data, support for the data reprocessing and bits of help along the way. Thanks to the sponsors of the OU Attribute-Assisted Seismic Processing and Interpretaion (AASPI) consortium. Thanks to Schlumberger for providing OU with licenses to Petrel used in the interpretation, ant-tracking, and 3D multi-attribute co-rendering.

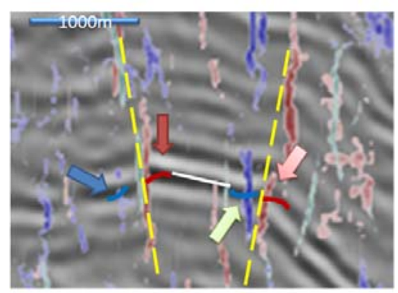

Figure 8: Intepreted faults (yellow) on a pop-up feature bound by coherence (green), maximum curvature (red), minimum curvature (blue) anomalies.

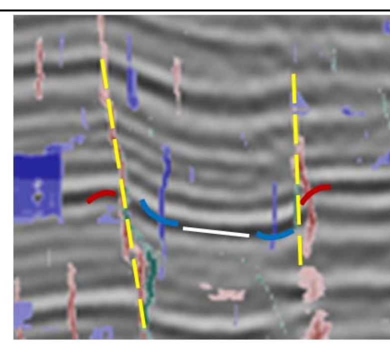

Figure 7: Interpreted faults (yellow) and intervening graben delineated by maximum curvature (red) and minimum curvature and coherence (green).

Coherence and volumetric curvatures and their spatial relationship to faults and folds, an example from Chicontepec basin, Mexico

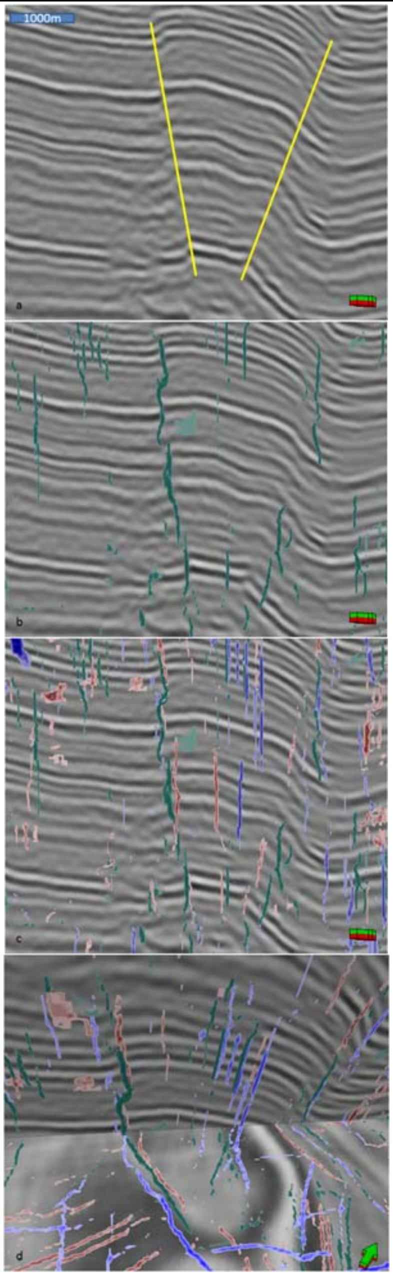

Figure 9: A representative seismic line with (a) interpreted faults, (b) coherence, (c) co-rendered ant-tracked maximum curvature, minimum curvature and coherence with the vertical seismic line, and (d) with an itersecting time slice as well. Intepreted faults (yellow) on a pop-up feature bound by coherence (green), maximum curvature (red), minimum curvature (blue) anomalies.

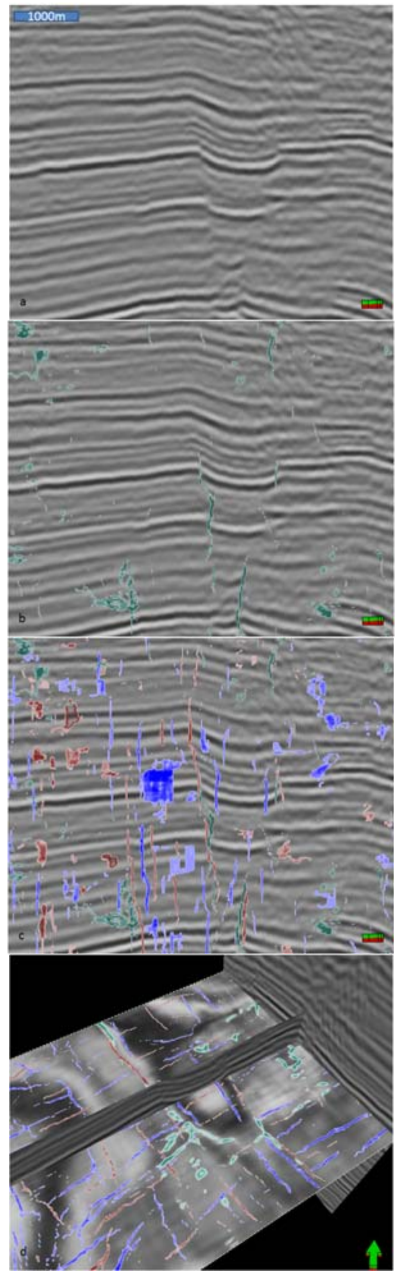

Figure 10: Interpreted faults (yellow) and intervening graben delineated by maximum curvature (red) and minimum curvature and coherence (green): (a) seismic line with interpreted fault (b) coherence, c) ant-tracked maximum curvature, minimum curvature and coherence on seismic line, d) their horizontally extend.